

Light scattering in Cooper-paired Fermi atoms

Bimalendu Deb

Physical Research Laboratory, Navrangpura, Ahmedabad 380 009, India

Abstract. We present a detailed theoretical study of light scattering off superfluid trapped Fermi gas of atoms at zero temperature. We apply Nambu-Gorkov formalism of superconductivity to calculate the response function of superfluid gas due to stimulated light scattering taking into account the final state interactions. The polarization of light has been shown to play a significant role in response of Cooper-pairs in the presence of a magnetic field. Particularly important is a scheme of polarization-selective light scattering by either spin-component of the Cooper-pairs leading to the single-particle excitations of one spin-component only. These excitations have a threshold of 2Δ where Δ is the superfluid gap energy. Furthermore, polarization-selective light scattering allows for unequal energy and momentum transfer to the two partner atoms of a Cooper-pair. In the regime of low energy ($\ll 2\Delta$) and low momentum ($< 2\Delta/(\hbar v_F)$, v_F being the Fermi velocity) transfer, a small difference in momentum transfers to the two spin-components may be useful in exciting Bogoliubov-Anderson phonon mode. We present detailed results on the dynamic structure factor (DSF) deduced from the response function making use of generalized fluctuation-dissipation theorem. Model calculations using local density approximation for trapped superfluid Fermi gas shows that when the energy transfer is less than $2\Delta_0$, where Δ_0 refers to the gap at the trap center, DSF as a function of energy transfer has reduced gradient compared to that of normal Fermi gas.

PACS numbers: 03.75.Ss,74.20.-z,32.80.Lg

1. Introduction

Cold atoms are of enormous research interest in current physics. The tremendous advancement in technology of cooling, trapping and manipulation [1] of atomic gases during 80's and 90's has enabled researchers to achieve a low temperature down to a few hundredth of a microKelvin. This led to the first realizations of Bose-Einstein condensation (BEC) [2] in dilute gases of ultracold bosonic atoms about a decade ago. Predicted in 1924 by Einstein [3] based quantum statistics of indistinguishable particles discovered by Bose [4], BEC in gaseous systems had long been thought a subject of mere academic pursuit beyond experimental reach because of the requirement of ultralow temperature which was unimaginable even two decades ago. The success in BEC is a breakthrough prompting researchers to look for experimental realizations of many other theoretical predictions of quantum physics using cold atoms. The most remarkable property of such atoms is the tunability of the atom-atom interaction over a wide range by an externally applied magnetic field or other means. This provides an unique opportunity to explore physics of interacting many-particle systems in a new parameter regime. In this context, the focus of attention has been now shifted to cold atoms obeying Fermi-Dirac statistics. Since fermions are the basic constituents of matter, research with Fermi atoms under controlled physical conditions has important implications in the entire spectrum of physical and chemical sciences. In particular, it has significant relevance in the field of superconductivity [5, 6].

The quantum degeneracy in an atomic Fermi gas was first realized by Jin's group [7] in 1999. Since then, cold Fermi atoms have been in focus of research interest in physics today. In a series of experiments, several groups [8, 9, 10, 11, 12, 13] have demonstrated many new aspects of degenerate atomic Fermi gases. In a remarkable recent experiment, Ketterle's group [14] has realized quantized vortices as a signature of Fermi superfluidity in a trapped atomic gas. Two groups-Innsbruck [15] and JILA [16] have independently reported the measurement of pairing gap in Fermi atoms. Furthermore, Duke and Innsbruck groups [17, 18] have measured collective oscillations which indicate the occurrence of superfluidity [19]. One of the key issues in this field is the crossover [20, 21, 22] between BCS state of atoms and BEC of molecules formed from Fermi atoms. Several groups have demonstrated BEC [23] of molecules formed from degenerate Fermi gas. There have been many other experimental [24] and theoretical investigations [25] revealing many intriguing aspects of interacting Fermi atoms.

The analysis of response of Cooper-paired Fermi atoms due to external perturbation (such as photon or rf field) is important for understanding the nature of atomic Fermi superfluid. A method has been suggested to use resonant light [26] to excite one of the spin components into an excited electronic state and thereby making an interface between normal and superfluid atoms. This is analogous to superconductive tunnelling which has a threshold equal to the gap energy Δ . This has been recently implemented (albeit using rf field) [15, 27] to estimate gap energy. There have been several other proposals [26, 28] for probing pairing gap.

Our purpose here is to calculate response function of superfluid Fermi gas due to stimulated light scattering that does not cause any electronic excitation in the atoms. We particularly emphasize the role of light polarization in single-particle excitations which have a threshold 2Δ . We present a scheme by which it is possible to have single-particle excitation in only one partner atom (of a particular hyperfine spin state) of a Cooper-pair using proper light polarizations in the presence of a magnetic field. This may lead to better precision in spin-selective time-of-flight detection of scattered atoms. Furthermore, spin-selective light scattering allows for unequal energy and momentum transfer into the two partner atoms of a Cooper-pair. This may be useful in exciting Bogoliubov-Anderson (BA) phonon mode of symmetry breaking by making small difference in momentum transfers received by the two partner atoms from the photon fields. A number of authors [29, 30, 31] have theoretically investigated Bogoliubov-Anderson (BA) mode [32, 33, 34] in fermionic atoms as a signature of superfluidity. BA mode constitutes a distinctive feature of superfluidity in neutral Fermi systems since it is associated with long wave Cooper-pair density fluctuations. However, experimental detection of this mode is a challenging problem.

We present a detailed theoretical analysis of the response function of Cooper-paired atoms at zero temperature due to light scattering. The stimulated light scattering we discuss here is similar to Bragg spectroscopy used by Ketterle's group for measuring structure factor of an atomic BEC [35]. The response function we derive is applicable for most general case of polarization-selective single-particle excitations for unequal (or equal) momentum as well as energy transfers to the two partner atoms of a Cooper-pair. We develop the theoretical framework for stimulated light scattering off Cooper-paired Fermi atoms following the method used for describing Raman scattering in superconductors [36, 37]. We use standard Nambu-Gorkov formalism of superconductivity [39, 38] to calculate the response function taking into account the vertex correction due to final state interactions. We deduce dynamic structure factor (DSF) from the response function applying generalized fluctuation-dissipation theorem. We present detailed analytical and numerical results of our calculation of DSF of trapped superfluid Fermi gas of atoms using local density approximation. The inhomogeneity of trapped gas has a role in distinguishing the DSF of superfluid gas from that of normal gas. When the energy transfer is smaller than $2\Delta_0$ where Δ_0 is the gap at the trap center, the DSF of superfluid gas as a function of energy transfer shows much reduced gradient in comparison to that of normal gas. This is because of the fact that the gap Δ has an inhomogeneous distribution gradually vanishing at the edge of the trap.

The paper is organized in the following way. In the following two sections, we define bare vertex in light scattering and response function, respectively. In the fourth section, we discuss stimulated light scattering in two-component ${}^6\text{Li}$ Fermi atoms in the presence of a magnetic field. We next describe in detail the method of vertex correction in light scattering off Cooper-paired Fermi atoms. In the sixth section, we discuss our analytical results followed by description on numerical results in the seventh section, and then we conclude.

2. Bare vertex in light scattering

To begin with, let us consider an elementary process of photon scattering by a neutral atom. Let the atom's initial and scattered electronic state be denoted by A and B , respectively. The frequencies of the incident and scattered photon are represented by ω_1 and ω_2 , respectively. According to second order perturbation theory, the strength of scattering is given by Kramers-Heisenberg formula [40]

$$\gamma_{BA} = \delta_{AB} \hat{\epsilon}_1 \cdot \hat{\epsilon}_2 - \frac{1}{m_e \hbar} \sum_I \left[\frac{(\mathbf{p} \cdot \hat{\epsilon}_2)_{BI} (\mathbf{p} \cdot \hat{\epsilon}_1)_{IA}}{\omega_{IA} - \omega_1} + \frac{(\mathbf{p} \cdot \hat{\epsilon}_1)_{BI} (\mathbf{p} \cdot \hat{\epsilon}_2)_{IA}}{\omega_{IA} + \omega_2} \right], \quad (1)$$

where I denotes all the intermediate atomic states that can be coupled to the initial and final atomic states A and B by the incident and scattered photon fields. Here \mathbf{p} and m_e are the momentum and mass of the valence electron of atom, $\hat{\epsilon}_{1(2)}$ denotes the polarization state of the incident (scattered) photon, ω_{IA} is the atomic frequency between the states I and A . The atomic transition ($A \rightarrow B$) probability and the differential scattering cross section of photons is proportional to $|\gamma|^2$ [40]. It should be mentioned that γ does not depend on the momentum transfer \mathbf{q} associated with the scattering, but it is sensitive to light polarization directions. Let us now consider the particular case: $A = B$ that is, before and after the scattering, the atom remains in the same electronic state. Then, making use of the completeness of the intermediate states I , one can rewrite the term $\hat{\epsilon}_1 \cdot \hat{\epsilon}_2$ as [40]

$$\hat{\epsilon}_1 \cdot \hat{\epsilon}_2 = \frac{1}{m_e \hbar} \sum_I \frac{1}{\omega_{IA}} [(\mathbf{p} \cdot \hat{\epsilon}_2)_{AI} (\mathbf{p} \cdot \hat{\epsilon}_1)_{IA} + (\mathbf{p} \cdot \hat{\epsilon}_1)_{AI} (\mathbf{p} \cdot \hat{\epsilon}_2)_{IA}], \quad (2)$$

Further, let us assume $\omega_1 \simeq \omega_2 \simeq \omega_{IA}$, that is, the incident as well as scattered light fields are in near resonance with the atomic frequency. In such a case, the second term within the third bracket on the right hand side (RHS) of Eq. (1) is much smaller than the first term, because energy denominator of the second term is of the order of optical frequency while that of the first term can be chosen to be smaller by several orders of magnitude. Thus, neglecting the second term, the bare vertex can be written as [40]

$$\gamma_{AA} = -\frac{1}{m_e \hbar} \sum_I \frac{\omega_1 (\mathbf{p} \cdot \hat{\epsilon}_2)_{AI} (\mathbf{p} \cdot \hat{\epsilon}_1)_{IA}}{\omega_{IA} (\omega_{IA} - \omega_1)}. \quad (3)$$

Next, using electric-dipole approximation and the fact $\omega_1/\omega_{IA} \simeq 1$, one can express

$$\gamma_{AA} = \Omega_0^{-1} \sum_I \frac{(\mathbf{d}_{AI} \cdot \hat{\mathcal{E}}_2)(\mathbf{d}_{AI} \cdot \hat{\mathcal{E}}_1)}{\hbar^2 (\omega_{AI} - \omega_1)} \quad (4)$$

where \mathbf{d}_{AI} is the transition dipole moment between the states A and I , $\hat{\mathcal{E}}_i = \mathcal{E}_i \hat{\epsilon}_i$ is the electric field and

$$\Omega_0 = \frac{e^2 \mathcal{E}_1 \mathcal{E}_2}{m_e \sqrt{n_1} \hbar \omega_1 \omega_2} \quad (5)$$

with n_1 being the number of incident photons.

3. The response function

To define response function of fermionic atoms due to an applied laser field, we use the second-quantized operator $a_{\sigma,\mathbf{k}}(a_{\sigma,\mathbf{k}}^\dagger)$ which describes the annihilation(creation) of an atom with hyperfine spin σ and center-of-mass momentum \mathbf{k} . These operators satisfy fermionic algebra. The effective atom-field hamiltonian is $H_{eff} = H_0 + H_I$, where

$$H_0 = \sum_{\sigma,\mathbf{k}} \hbar(\omega_k - \delta) a_{\sigma,\mathbf{k}}^\dagger a_{\sigma,\mathbf{k}}, \quad \omega_k = \frac{\hbar k^2}{2m}, \quad (6)$$

with $\delta = \omega_1 - \omega_2$ being the frequency-difference between incident and scattered photons. We assume that, except the center-of-mass momentum, the spin or any other internal degrees of atom does not change due to light scattering. By treating light fields classically, the effective interaction hamiltonian can then be written as

$$H_I = \hbar\Omega_0 \sum_{\sigma,\mathbf{k}} \gamma_{\sigma\sigma} a_{\sigma,\mathbf{k}+\mathbf{q}}^\dagger a_{\sigma,\mathbf{k}} + \text{H.c.} \quad (7)$$

where \mathbf{q} is the momentum transferred to the atom due to photon scattering and $\gamma_{\sigma\sigma}$ represents the bare vertex corresponding to the ground hyperfine spin magnetic quantum number σ .

Now, one can define the density operators by $\rho_q^{(0)} = \sum_{\sigma,\mathbf{k}} a_{\sigma,\mathbf{k}+\mathbf{q}}^\dagger a_{\sigma,\mathbf{k}}$ and

$$\rho_q^{(\gamma)} = \sum_{\mathbf{k},\sigma} \gamma_{\sigma\sigma} a_{\sigma,\mathbf{k}+\mathbf{q}}^\dagger a_{\sigma,\mathbf{k}} \quad (8)$$

One can identify the operator $\rho_q^{(0)}$ as the Fourier transform of the density operator in real space. The scattering probability of incident particles (photons in the present context) is related to the response or susceptibility

$$\chi(\mathbf{q}, \tau - \tau') = -\langle T_\tau [\rho_q^{(\gamma)}(\tau) \rho_{-q}^{(\gamma)}(\tau')] \rangle \quad (9)$$

of the target system by which the incident particles are scattered. Here $\langle \dots \rangle$ means thermal averaging and T_τ is the complex time τ ordering operator. The Fourier transform of this susceptibility is

$$\chi(\mathbf{q}, \omega_n) = \frac{1}{2} \int_{-T}^T d\tau e^{i\omega_n \tau} \chi(\mathbf{q}, \tau) \quad (10)$$

where T is the temperature and $\omega_n = 2\pi nT$ is the Matsubara frequency with n being an integer. The scattering cross section is proportional to the generalized dynamic structure factor which can be obtained by the generalized fluctuation-dissipation theorem through the analytic continuation of $\chi(\mathbf{q}, \omega_n)$ as

$$S(\mathbf{q}, \omega) = -\frac{1}{\pi} [1 + n_B(\omega)] \text{Im}[\chi(\mathbf{q}, z = \omega + i\delta)]. \quad (11)$$

We define the following polarization matrix element:

$$\Pi_{ij}(\mathbf{q}, \tau - \tau') = -\langle T_\tau [\rho_q^{(i)}(\tau) \rho_{-q}^{(j)}(\tau')] \rangle \quad (12)$$

where $i, j \equiv \gamma, 0$. The polarization bubble $\Pi_{\gamma\gamma}$ is nothing but the susceptibility $\chi(\mathbf{q}, \tau - \tau')$ of Eq. (9). The dynamic structure factor is thus related to this polarization term by fluctuation-dissipation relation as expressed in Eq. (11). The spectrum of density fluctuation is proportional to the dynamic structure factor which can also be defined as the Fourier transform of the two-time density-density correlation function.

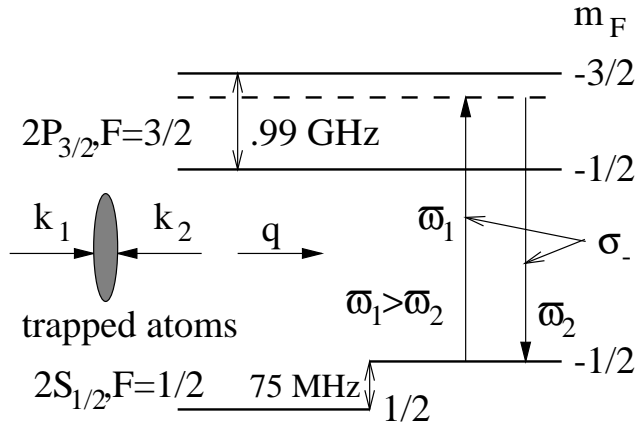


Figure 1. A schematic level diagram for polarization-selective light scattering in two-component Fermi gas of ${}^6\text{Li}$ atoms

4. stimulated light scattering in two-component Fermi atoms

We would like to study stimulated light scattering in two-component Fermi atoms. In particular, we consider trapped ${}^6\text{Li}$ Fermi atoms in their two lowest hyperfine spin states $|g\rangle_1 = |2S_{1/2}, F = 1/2, m_F = 1/2\rangle \equiv |\uparrow\rangle$ and $|g\rangle_2 = |2S_{1/2}, F = 1/2, m_F = -1/2\rangle \equiv |\downarrow\rangle$. For simplicity, the number of atoms in each spin component is assumed to be the same. However, a mismatch in number densities of the two spin components may lead to interior gap superfluidity [41, 42] in a Fermi gas of atoms. An applied magnetic field tuned near the Feshbach resonance (~ 850 Gauss) results in splitting between the two spin states by ~ 75 MHz [43], while the corresponding splitting between the excited states $|e\rangle_1 = |2P_{3/2}, F = 3/2, m_F = -1/2\rangle$ and $|e\rangle_2 = |2P_{3/2}, F = 3/2, m_F = -3/2\rangle$ is ~ 994 MHz [10].

Figure 1 shows the schematic level diagram for stimulated light scattering by two-component ${}^6\text{Li}$ atoms. Two off-resonant laser beams with a small frequency difference are impinging on atoms, the scattering of one laser photon is stimulated by the other photon. In this process, one laser photon is annihilated and reappeared as a scattered photon propagating along the other laser beam. The magnitude of momentum transfer is $q \simeq 2k_L \sin(\theta/2)$, where θ is the angle between the two beams and k_L is the momentum of a laser photon. Let both the laser beams be σ_- polarized and tuned near the transition $|g\rangle_2 \rightarrow |e\rangle_2$. Then the transition between the states $|g\rangle_1$ and $|e\rangle_2$ would be forbidden while the transition $|g\rangle_1 \rightarrow |e\rangle_1$ will be suppressed due to the large detuning ~ 900 MHz. This leads to a situation where the scattered atoms remain in the same initial internal state $|g\rangle_2$. Similarly, atoms in state $|g\rangle_1$ only suffer scattering when two σ_+ polarized lasers are tuned near the transition $|g\rangle_1 \rightarrow |2P_{3/2}, F = 3/2, m_F = 3/2\rangle$. Thus, it is possible to scatter atoms selectively of either spin components using circularly polarized lasers in the presence of magnetic field. Under such conditions, considering a uniform gas of atoms, the effective laser-atom interaction Hamiltonian in electric-dipole

approximation can be written as

$$H_I = \hbar\Omega_0 \sum_{\mathbf{k}, \sigma=\uparrow, \downarrow} \gamma_{\sigma\sigma} a_{\sigma, \mathbf{k}+\mathbf{q}}^\dagger a_{\sigma, \mathbf{k}} + \text{H.c.} \quad (13)$$

If σ refers to $|\downarrow\rangle$ then

$$\gamma_{\sigma\sigma} = \Omega_0^{-1} \sum_{i=1,2} \frac{(\mathbf{d}_{22} \cdot \hat{\mathcal{E}}_2)(\mathbf{d}_{22} \cdot \hat{\mathcal{E}}_1)}{\hbar^2(\omega_{22} - \omega_i)}. \quad (14)$$

where d_{ii} is the transition dipole matrix element between the ground $|g\rangle_i$ and the excited $|e\rangle_i$ states. Similarly, if σ is $|\uparrow\rangle$ then the subscript “22” should be replaced by “11”. In writing the above vertex term, we have also assumed that both the laser beams are of almost equal intensity. For both the laser beams having σ_- polarization tuned near $|g\rangle_2 \rightarrow |e\rangle_2$ as in Fig. 1, one finds $\gamma_{\downarrow\downarrow} \gg \gamma_{\uparrow\uparrow}$. On the other hand, in the absence of magnetic field (or in the presence of a weak magnetic field), the hyperfine magnetic sub-levels of the ground and excited state would be degenerate (or nearly degenerate). In such a case, irrespective of whether both the laser beams are unpolarized or equally polarized, we have $\gamma_{\uparrow\uparrow} \simeq \gamma_{\downarrow\downarrow}$.

5. light scattering in Cooper-paired Fermi atoms: Vertex correction

To study light scattering in Cooper-paired Fermi atoms, we apply Nambu-Gorkov formalism that uses the four Pauli matrices

$$\tau_0 = \begin{pmatrix} 1 & 0 \\ 0 & 1 \end{pmatrix}, \quad \tau_1 = \begin{pmatrix} 0 & 1 \\ 1 & 0 \end{pmatrix}, \quad \tau_2 = \begin{pmatrix} 0 & -i \\ i & 0 \end{pmatrix}, \quad \tau_3 = \begin{pmatrix} 1 & 0 \\ 0 & -1 \end{pmatrix} \quad (15)$$

The vertex equation is [44]

$$\Gamma(k_+, k_-) = \tilde{\gamma} + i \int \frac{d^4 k'}{(2\pi)^4} \tau_3 \mathbf{G}(k'_+) \Gamma(k'_+, k'_-) \mathbf{G}(k'_-) \tau_3 V(\mathbf{k}, \mathbf{k}'), \quad (16)$$

where $k_\pm = k \pm q/2$ and $k = (\mathbf{k}, k_0)$ is the energy-momentum 4-vector whose components are $k_3 = \xi_k$ and $k_4 = ik_0$. In pairing approximation, the Green function can be expressed in a matrix form as

$$G(k) = \frac{k_0 \tau_0 + \xi_k \tau_3 + \Delta_k \tau_1}{k_0^2 - E_k^2 + i\delta}, \quad (17)$$

where $E_k = \sqrt{\xi_k^2 + \Delta_k^2}$ and $\xi_k = \epsilon_k - \mu$ with $\epsilon_k = \hbar^2 k^2 / (2m)$. The bare vertex

$$\tilde{\gamma} = \begin{pmatrix} \gamma_{\uparrow\uparrow} & 0 \\ 0 & -\gamma_{\downarrow\downarrow} \end{pmatrix}. \quad (18)$$

Using Pauli matrices τ_0 and τ_3 , this can be rewritten as

$$\tilde{\gamma} = \gamma_0 \tau_0 + \gamma_3 \tau_3, \quad (19)$$

where $\gamma_0 = [\gamma_{\uparrow\uparrow} - \gamma_{\downarrow\downarrow}] / 2$ and $\gamma_3 = [\gamma_{\uparrow\uparrow} + \gamma_{\downarrow\downarrow}] / 2$. The susceptibility is given by

$$\chi(\mathbf{q}, \omega) = \int \frac{d^4 k}{(2\pi)^4 i} \text{Tr}[\tilde{\gamma}_k \mathbf{G}(k_+) \Gamma(k_+, k_-) \mathbf{G}(k_-)] \quad (20)$$

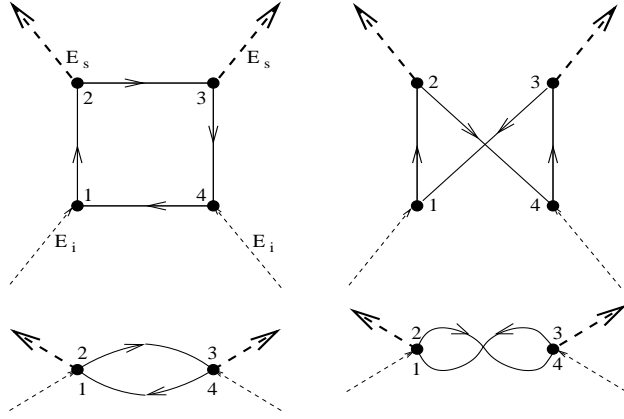


Figure 2. The upper part shows two irreducible four-vertex diagrams of stimulated light scattering off noninteracting normal Fermi gas of atoms. The thin dashed lines with arrows represent the incident laser field (with electric field \mathbf{E}_i) and the thick dashed lines refer to the emitted photon stimulated by another laser field (\mathbf{E}_s). The operators $\mathbf{d}\cdot\mathbf{E}_i$ and $\mathbf{d}\cdot\mathbf{E}_s$ act at the vertex pairs (1,4) and (2,3), respectively; where \mathbf{d} is the transition dipole moment between the ground $|g_1\rangle$ ($|g_2\rangle$) and the excited $|e_1\rangle$ ($|e_2\rangle$) state. The vertex pair (1,2) can be replaced by an effective single vertex where the operator $\gamma_{\sigma\sigma}\rho_q$ acts, where $\gamma_{\sigma\sigma}$ is given as in Eq. (14). Similarly, the pair (3,4) can be combined to form an effective vertex. Thus, the four vertex diagrams effectively reduce to bubble diagrams as shown in the lower part. Note that the role of incident and scattered fields can be reversed, since an atom can absorb a photon from the laser mode marked “ \mathbf{E}_s ” and emit into the mode marked “ \mathbf{E}_i ”. By treating laser fields classically, the effective vertex operators can be expressed only in terms of atomic Fermi operators as in Eq. (13).

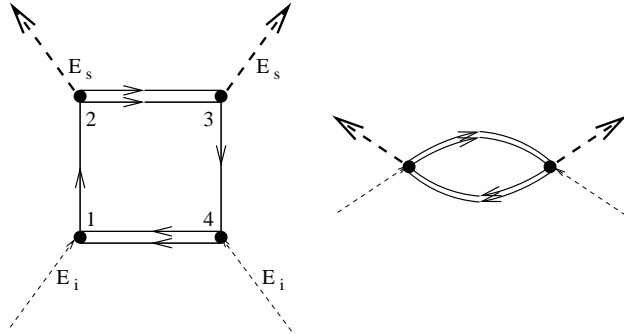


Figure 3. An irreducible four-vertex diagrams of stimulated light scattering in an atomic Fermi superfluid when the quasi-particles are assumed to be noninteracting. The double lines with arrows represent Nambu propagator for Cooper pairs. As in Fig 2, the four vertex diagram can be effectively represented by a two-vertex bubble diagram.

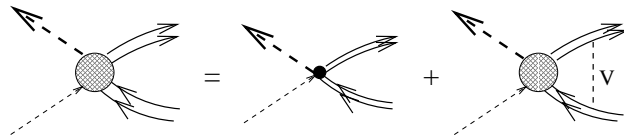


Figure 4. Diagrammatic representation of vertex equation

5.1. vertex equation and its solution

To solve the vertex equation, let us expand the vertex function in terms of Pauli matrices as

$$\Gamma(k_+, k_-) = \sum_{i=0}^3 \Gamma^{(i)}(\mathbf{k}, \mathbf{q}, \omega) \tau_i. \quad (21)$$

Using Eqs. (17) and (21) in Eq. (16), we can write

$$\Gamma(\mathbf{k}, \mathbf{q}, \omega) = \tilde{\gamma}_k + i \int \frac{d^4 k'}{(2\pi)^4} V(\mathbf{k}, \mathbf{k}') \frac{1}{(k'_+{}^2 + \Delta_{k'}^2)(k'_-{}^2 + \Delta_{k'}^2)} \sum_{i=0}^3 y_i \tau_i, \quad (22)$$

where $k^2 = k_3^2 + k_4^2 = \xi_k^2 - k_0^2$ and

$$\begin{aligned} y_0 &= [k'_{+0} \epsilon_{k'_-} + k'_{-0} \epsilon_{k'_+}] \Gamma^{(3)} - i \Delta_{k'} [\epsilon_{k'_+} - \epsilon_{k'_-}] \Gamma^{(2)} + \Delta_{k'} [k'_{+0} + k'_{-0}] \Gamma^{(1)} \\ &\quad + [\epsilon_{k'_+} \epsilon_{k'_-} + k'_{+0} k'_{-0} + \Delta_{k'}^2] \Gamma^{(0)}, \\ y_1 &= -i [k'_{+0} \epsilon_{k'_-} - k'_{-0} \epsilon_{k'_+}] \Gamma^{(2)} - \Delta_{k'} [\epsilon_{k'_+} + \epsilon_{k'_-}] \Gamma^{(3)} - \Delta_{k'} [k'_{+0} + k'_{-0}] \Gamma^{(0)} \\ &\quad + [\epsilon_{k'_+} \epsilon_{k'_-} - k'_{+0} k'_{-0} - \Delta_{k'}^2] \Gamma^{(1)}, \\ y_2 &= -i \Delta_{k'} [k'_{+0} - k'_{-0}] \Gamma^{(3)} - i \Delta_{k'} [\epsilon_{k'_+} - \epsilon_{k'_-}] \Gamma^{(0)} - i [\epsilon_{k'_+} k'_{-0} - k'_{+0} \epsilon_{k'_-}] \Gamma^{(1)} \\ &\quad + [\epsilon_{k'_+} \epsilon_{k'_-} - k'_{+0} k'_{-0} + \Delta_{k'}^2] \Gamma^{(2)}, \\ y_3 &= \Delta_{k'} [\epsilon_{k'_+} + \epsilon_{k'_-}] \Gamma^{(1)} - i \Delta_{k'} [k'_{+0} - k'_{-0}] \Gamma^{(2)} + [\epsilon_{k'_+} \epsilon_{k'_-} + k'_{+0} k'_{-0} - \Delta_{k'}^2] \Gamma^{(3)} \\ &\quad + [\epsilon_{k'_+} k'_{-0} + k'_{+0} \epsilon_{k'_-}] \Gamma^{(0)}. \end{aligned}$$

In writing the above equations, we have assumed $\Delta_{k_\pm} \simeq \Delta_k$. Further, we can write $\epsilon_{k_\pm} = \xi_k \pm \mathbf{v}_k \cdot \mathbf{p}_q / 2 + \epsilon_q$, where $\mathbf{v}_k = \hbar \mathbf{k} / m$, $\mathbf{p}_q = \hbar \mathbf{q}$ and $\epsilon_q = p_q^2 / (2m)$

Before performing the integration of Eq. (22), we note that the dominant contribution to the integral comes from k -values near $\xi_k \simeq 0$, that is, $\hbar^2 k^2 / (2m) \simeq \mu$. Hence we can approximate

$$\int \frac{d^4 \mathbf{k}}{(2\pi)^4} \simeq \int \frac{d^3 \mathbf{k}}{(2\pi)^3} \delta(\xi_k) \int \frac{dk_3 dk_0}{2\pi} \quad (23)$$

where $k_3 \equiv \xi_k$ denotes the third component of energy-momentum 4-vector $k = (\mathbf{k}, k_0)$. If the potential $V(\mathbf{k}, \mathbf{k}')$ is separable in two variables \mathbf{k} and \mathbf{k}' , then Eq. (16) is analytically solvable. Let us, for simplicity, replace $V(\mathbf{k}, \mathbf{k}')$ by the well-known mean field potential $V_{mf} = g a_s$ (where $g = 4\pi \hbar^2 / (2m)$) which is expressed in terms of s-wave scattering length a_s . By doing so, we are basically considering the weak-coupling case. However, within mean-field approximation the strong-coupling limit may be accessed by first renormalizing the BCS mean-field interaction and then taking the limit $a_s \rightarrow \pm\infty$ as will be discussed later.

With the assumption of a k -independent gap Δ , the double integrations on k_0 and k_3 then resemble to those appearing in relativistic equations in QED and so can be

carried out analytically by Feynman's method [45]. The angular integration is left to the last. There are basically two types of integrals:

$$I(q) = -i \int \frac{\Delta^2 dk_0 dk_3}{(k_+^2 + \Delta^2)(k_-^2 + \Delta^2)} \quad (24)$$

$$I_{ij}(q) = -i \int \frac{(k_+)_i (k_-)_j dk_0 dk_3}{(k_+^2 + \Delta^2)(k_-^2 + \Delta^2)}, \quad i, j = 3, 4 \quad (25)$$

These integrals are explicitly calculated in Ref. [46] using Feynman's method of parametrization. For completeness, we here reproduce the method of calculation. The terms which are odd in k will not contribute to the integration and so those terms can be omitted. Substituting $k = \tilde{k} - (q/2 - qx)$ where x is a parameter varying between 0 to 1, the integral of Eq. (24) can be reexpressed as

$$I = -i \int_0^1 dx \int \frac{\Delta^2 d\tilde{k}_0 d\tilde{k}_3}{[\tilde{k}^2 + \Delta^2 + q^2(x - x^2)]^2}. \quad (26)$$

The k_0 -integration can be carried out by residue method of complex integration. The pole is $\tilde{k}_0 = \sqrt{\tilde{k}_3^2 + L}$, where $L = \Delta^2 + q^2(x - x^2)$. Since L has infinitesimally negative imaginary part, the pole lies in the lower half of the real axis. The residue is $-[4(\tilde{k}_3^2 + L)^{3/2}]^{-1}$. After performing \tilde{k}_3 - and x -integration, one obtains the result $I(q) = f(q)/2$, where

$$f(q) = \frac{\arcsin \beta}{\beta \sqrt{1 - \beta^2}}, \quad (27)$$

$$\beta^2 = \frac{\omega^2 - (\mathbf{v}_k \cdot \mathbf{p}_q)^2}{4\Delta^2}. \quad (28)$$

The k_3 -integration in Eq. (26) is divergent, therefore a cut-off frequency ω_c is required as the upper limit of integration. After having performed the integration, the vertex terms $\Gamma^{(i)}$ can be expressed as

$$\begin{aligned} \Gamma^{(0)} &= \gamma_0(k) - ga_s \int \frac{d^3 \mathbf{k}}{(2\pi)^3} \delta(\xi_k) \\ &\times \left[\frac{\omega(\mathbf{v}_k \cdot \mathbf{p}_q)(1-f)}{\omega^2 - (\mathbf{v}_k \cdot \mathbf{p}_q)^2} \Gamma^{(3)} - i \frac{\mathbf{v}_k \cdot \mathbf{p}_q f}{2\Delta} \Gamma^{(2)} + \frac{(\mathbf{v}_k \cdot \mathbf{p}_q)^2 (1-f)}{\omega^2 - (\mathbf{v}_k \cdot \mathbf{p}_q)^2} \Gamma^{(0)} \right] \end{aligned} \quad (29)$$

$$\Gamma^{(1)} = -ga_s \int \frac{d^3 \mathbf{k}}{(2\pi)^3} \delta(\xi_k) \left[\ln \frac{\omega_c}{|\Delta|} + (\beta^2 - 1)f \right] \Gamma^{(1)} \quad (30)$$

$$\begin{aligned} \Gamma^{(2)} &= -ga_s \int \frac{d^3 \mathbf{k}}{(2\pi)^3} \delta(\xi_k) \\ &\times \left[-i \frac{\mathbf{v}_k \cdot \mathbf{p}_q f}{2\Delta} \Gamma^{(0)} + \left\{ \ln \frac{\omega_c}{|\Delta|} + \beta^2 f \right\} \Gamma^{(2)} - i \frac{\omega f}{2\Delta} \Gamma^{(3)} \right] \end{aligned} \quad (31)$$

$$\begin{aligned} \Gamma^{(3)} &= \gamma_3(k) - ga_s \int \frac{d^3 \mathbf{k}}{(2\pi)^3} \delta(\xi_k) \\ &\times \left[-i \frac{\omega f}{2\Delta} \Gamma^{(2)} + \frac{(\mathbf{v}_k \cdot \mathbf{p}_q)^2 - \omega^2 f}{\omega^2 - (\mathbf{v}_k \cdot \mathbf{p}_q)^2} \Gamma^{(3)} + \frac{\omega(\mathbf{v}_k \cdot \mathbf{p}_q)(1-f)}{\omega^2 - (\mathbf{v}_k \cdot \mathbf{p}_q)^2} \Gamma^{(0)} \right] \end{aligned} \quad (32)$$

Since $\Gamma^{(1)}$ is decoupled from all other vertex terms including the bare ones (γ_i), we can set $\Gamma^{(1)} = 0$. Using the expansion of Eq. (21), the susceptibility can be written as

$$\begin{aligned} \chi(\mathbf{q}, \omega) = & -\frac{2(\Gamma^{(0)} - \gamma_0)}{ga_s} \gamma_0 + 2 \int \frac{d^3\mathbf{k}}{(2\pi)^3} \delta(\xi_k) \\ & \times \left[\frac{(\mathbf{v}_k \cdot \mathbf{p}_q)^2 - \omega^2 f}{\omega^2 - (\mathbf{v}_k \cdot \mathbf{p}_q)^2} \Gamma^{(3)} - \frac{i\omega f}{2\Delta} \Gamma^{(2)} + \frac{\omega(\mathbf{v}_k \cdot \mathbf{p}_q)(1-f)}{\omega^2 - (\mathbf{v}_k \cdot \mathbf{p}_q)^2} \Gamma^{(0)} \right] \gamma_3. \end{aligned} \quad (33)$$

We note that the dressed part of $\Gamma^{(0)}$ is proportional to the momentum transfer q , therefore we have $\Gamma^{(0)} \simeq \gamma_0(k)$ in the low momentum transfer regime, that is, for $q \ll \xi^{-1}$, where $\xi = \hbar v_F / (2\Delta)$ is the BCS coherence length. Introducing the variable $z = \cos \theta$, where θ is the angle between \mathbf{v}_k and \mathbf{p}_q , we can drop all the terms odd in z in the above equations, since upon integration over z those terms vanish. Thus $\Gamma^{(0)}$ also becomes decoupled while $\Gamma^{(2)}$ and $\Gamma^{(3)}$ form only two coupled equations which can be analytically solved.

5.2. gap equation

The gap equation can be obtained from Eq. (31) by setting \mathbf{q} and ω equal to zero and replacing $\Gamma^{(2)}$ by the gap parameter Δ . The resulting equation reads

$$\Delta = -ga_s \int \frac{d^3\mathbf{k}}{(2\pi)^3} \delta(\xi_k) \ln \frac{\omega_c}{|\Delta|} \Delta. \quad (34)$$

The cut-off frequency ω_c has been introduced ad-hoc to tackle the divergence problem for the time being. This needs to be eliminated by the method of regularization. To this end, we here recall that in carrying out the various momentum integration, we made an approximation: the integration was restricted near the chemical potential (which is nearly equal to Fermi energy in the weak coupling regime). To restore the actual gap equation, we here remove this approximation and let $\omega_c \rightarrow \infty$ and thus obtain

$$-\frac{1}{ga_s} = \frac{1}{2} \int \frac{d^3\mathbf{k}}{(2\pi)^3} \frac{1}{\sqrt{\xi_k^2 + \Delta^2}}. \quad (35)$$

The gap defined by this equation is however, divergent. To remove this divergence, we define regularized mean-field coupling by subtracting from the right hand side of Eq. (35) the zero field contribution (i.e., $\Delta = 0$ and $\mu = 0$). The resulting gap equation is

$$-\frac{1}{ga_s} = \frac{1}{2} \int \frac{d^3\mathbf{k}}{(2\pi)^3} \left[\frac{1}{\sqrt{\xi_k^2 + \Delta^2}} - \frac{1}{\epsilon_k} \right] \quad (36)$$

which yields convergent results. In the weak-coupling regime ($|a_s|k_F \ll 1$), $\mu \simeq \epsilon_F \propto n^{2/3}$. The strong-coupling regime ($|a_s|k_F > 1$) may be accessed by simultaneously solving for the interacting chemical potential μ from the single-spin BCS number-density equation

$$n = \frac{1}{6\pi^2} k_F^3 = \frac{1}{2} \int \frac{d^3\mathbf{k}}{(2\pi)^3} \left(1 - \frac{\xi_k}{\sqrt{\xi_k^2 + \Delta^2}} \right). \quad (37)$$

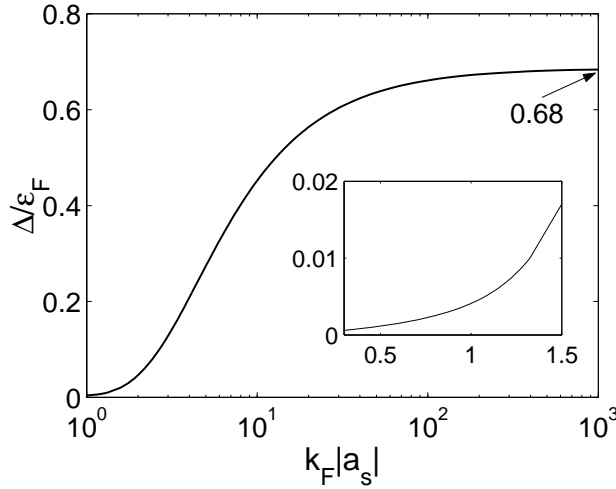


Figure 5. Gap Δ (in unit of ϵ_F) is plotted as a function of the dimensionless mean-field interaction parameter $k_F|a_s|$ on semi-logarithmic scale. The inset shows the same plot for small interaction parameter on linear scale. In the limit $k_F|a_s| \rightarrow \infty$, the gap saturates at a value $0.68 \epsilon_F$.

This approach of solving the regularized gap plus the number equation to access strong-coupling regime within the simple mean-field framework fails to account for pairing fluctuation effects which are particularly significant near T_c in the strong-coupling regime. However, far below T_c , the correction due to the pairing fluctuation is very small as shown in Ref. [21]. The two coupled Eqs. (36) and (37) admit analytical solutions which are obtained by Marini *et al.* [47] for the entire range of the parameter $a_s k_F$ starting from weak interaction ($a_s k_F \rightarrow \pm 0$) to the unitarity limit ($a_s k_F \rightarrow \pm \infty$). In the unitarity limit, the solutions provide $\mu = 0.59\epsilon_F$ and $\Delta \simeq 1.16\mu$. For convenience in solving the two coupled equations numerically, we rewrite the equations in terms of the two dimensionless scaled variables $x = k/k_\mu$ and $y = \Delta/\mu$ as

$$\frac{2\pi}{k_\mu|a_s|} = \int_0^\infty x^2 \left[\frac{1}{\sqrt{(x^2 - 1)^2 + y^2}} - \frac{1}{x^2} \right] dx \quad (38)$$

$$\left(\frac{k_F}{k_\mu} \right)^3 = \frac{3}{2} \int_0^\infty x^2 \left[1 - \frac{x^2 - 1}{\sqrt{(x^2 - 1)^2 + y^2}} \right] dx \quad (39)$$

where $k_\mu = \sqrt{2m\mu}/\hbar$. We have set $a_s = -|a_s|$. Calling the right hand side of Eqs. (38) and (39) as I_1 and I_2 , respectively; eliminating k_μ from both the equations, we obtain

$$\frac{2\pi}{k_F|a_s|} = \frac{I_1}{(I_2)^{1/3}}. \quad (40)$$

For given values of the parameters k_F and $|a_s|$, the Eq. (40) can be solved for y . Then substituting this solution into Eq. (38), one evaluates μ and so also the gap $\Delta = \mu y$

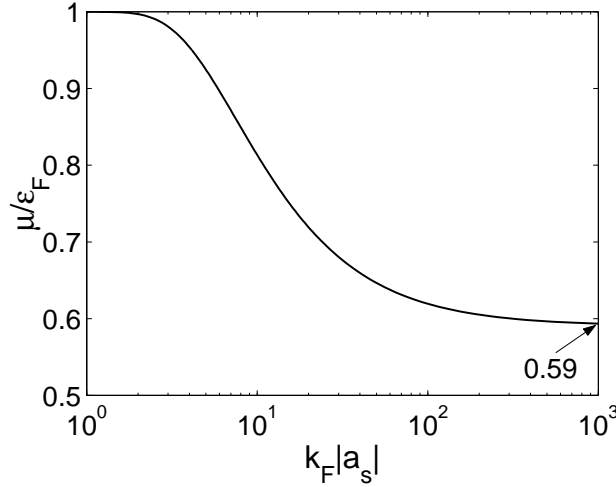


Figure 6. Chemical potential μ (in unit of ϵ_F) is plotted against parameter $k_F|a_s|$. In the limit $k_F|a_s| \rightarrow \infty$, μ saturates at a value $0.59 \epsilon_F$. In the limit $k_F|a_s| \rightarrow 0$, μ goes to unity.

5.3. solutions

Now, to write down the solutions of the various vertex terms $\Gamma^{(i)}$ and the susceptibility χ is straightforward. Let $\kappa_s = N(0)ga_s$, where $N(0) = (\pi^2\hbar^2)^{-1}mk_F$ represents the single particle density of states near the chemical potential. The various vertex terms can be expressed as

$$\Gamma^{(3)} = \frac{\gamma_3}{1 + \kappa_s F}, \quad (41)$$

$$\Gamma^{(2)} = \frac{i\omega\langle f \rangle}{2\Delta\langle \beta^2 f \rangle} \Gamma^{(3)}, \quad (42)$$

and

$$\Gamma^{(0)} = \frac{\gamma_0}{1 + \kappa_s \langle B \rangle}. \quad (43)$$

Here

$$F = \langle A \rangle + \frac{\omega^2 \langle f \rangle^2}{4\Delta^2 \langle \beta^2 f \rangle}, \quad (44)$$

$$A = \frac{(\mathbf{v}_k \cdot \mathbf{p}_q)^2 - \omega^2 f}{\omega^2 - (\mathbf{v}_k \cdot \mathbf{p}_q)^2}, \quad (45)$$

and

$$B = \frac{(\mathbf{v}_k \cdot \mathbf{p}_q)^2 (1 - f)}{\omega^2 - (\mathbf{v}_k \cdot \mathbf{p}_q)^2}. \quad (46)$$

The symbol $\langle X \rangle$ implies average of a function X over the chemical potential surface: $\langle X \rangle = [N(0)]^{-1} \int d^3\mathbf{k} \delta(\epsilon_k) X$, since X is an even function of $z = \cos \theta$, we have

$\langle X \rangle = (1/2) \int_0^1 X(k_F, z) dz$. Making use of these vertex terms, the susceptibility can be written as

$$\chi(\mathbf{q}, \omega) = 2N(0) \frac{\gamma_0^2 \langle B \rangle}{1 + \kappa_s \langle B \rangle} + 2N(0) \left[\gamma_3^2 F - \frac{\kappa_s \gamma_3 F^2}{1 + \kappa_s F} \right] \quad (47)$$

We drop the second term inside the third bracket which leads to small corrections due to Landau-liquid-like behavior without adding any significant qualitative effect. Further, for $\kappa_s \langle B \rangle \ll 1$, we have

$$\chi(\mathbf{q}, \omega) = 2N(0) \left[\gamma_0^2 \langle B \rangle + \gamma_3^2 F \right] \quad (48)$$

6. dynamic structure factor

The dynamic structure factor is obtained from the response function χ via analytic continuation of energy $\omega \rightarrow \omega + i0^+$. By means of generalized fluctuation-dissipation theorem as embodied in Eq. (11), in the zero temperature limit the dynamic structure factor is related to the imaginary part of the density response function χ via analytic continuation of energy $\omega \rightarrow \omega + i0^+$ as

$$S(\mathbf{q}, \omega) = -\frac{1}{\pi} \text{Im}[\chi(\mathbf{q}, \omega \rightarrow \omega + i0^+)]. \quad (49)$$

The key function here is $f(\beta)$ of Eq. (27), where β is given in Eq. (28). As $\omega \rightarrow \omega + i0^+$, $\beta \rightarrow \beta + i0^+$. We have the following analytic properties of $f(\beta)$:

$$f(\beta) = h(\beta) + \frac{i\pi/2}{\beta\sqrt{\beta^2 - 1}}, \quad \beta > 1 \quad (50)$$

where

$$h = -\frac{\text{arcsinh}\sqrt{\beta^2 - 1}}{\beta\sqrt{\beta^2 - 1}} \quad (51)$$

The use of Eqs. (44), (45) and (46) in Eq. (48) which, along with Eq. (50), on being substituted in Eq. (49) leads to the result

$$S(\mathbf{q}, \omega) = \gamma_0^2 S_0(\mathbf{q}, \omega) + \gamma_3^2 S_3(\mathbf{q}, \omega) \quad (52)$$

where

$$S_0(\mathbf{q}, \omega) = N(0) \frac{\omega^2}{4\Delta^2} \left\langle \frac{(\mathbf{p}_q \cdot \mathbf{v}_F)^2}{\beta^3 \sqrt{\beta^2 - 1}} \right\rangle \quad (53)$$

$$\begin{aligned} S_3(\mathbf{q}, \omega) = & N(0) \frac{\omega^2}{4\Delta^2} \left\langle \frac{1}{\beta^3 \sqrt{\beta^2 - 1}} \right\rangle - N(0) \frac{\omega^2}{4\Delta^2} \frac{1}{|\langle \beta^2 f \rangle|^2} \\ & \times \left\{ \left\langle \frac{2\langle h \rangle \langle \beta^2 h \rangle}{\beta \sqrt{\beta^2 - 1}} \right\rangle - \text{Re}[\langle f \rangle^2] \left\langle \frac{\beta}{\sqrt{\beta^2 - 1}} \right\rangle \right\} \end{aligned} \quad (54)$$

7. Analytical results and discussions

Equation (52) gives an expression for dynamic structure factor of a homogeneous Fermi superfluid when the excitations are of single-particle type for the parameters satisfying $\beta > 1$. Different amount of energy transfers (or excitations) to the two constituent partners of a broken Cooper-pair can be made by appropriately selecting the polarization states of the exciting two laser beams and tuning their frequency from the excited atomic state in the presence of a magnetic field. This fact is taken into account in the expression of (52), because any nonzero value of the term γ_0 means unequal excitation of the two partners. For instance, two extreme cases can be mentioned: Case-I: For unpolarized light in the absence of magnetic field, equal amount of energy transfer occurs to the two partners resulting in $\gamma_0 = 0$; Case-II: On the other hand, for circularly polarized light in the presence of strong magnetic field, we have $\gamma_0^2 \simeq \gamma_3^2$ meaning only either partner can be excited. We will present our numerical results for these two extreme cases. To compare our results with the known results for normal Fermi system in the limit $\Delta \rightarrow 0$, we will use in Case-I the limit $\gamma_{\uparrow\uparrow} \simeq \gamma_{\downarrow\downarrow} \rightarrow 1$ meaning $\gamma_0 \rightarrow 0$ and $\gamma_3 \rightarrow 1$. In Case-II, we will use the limit $\gamma_{\uparrow\uparrow} \simeq 0$ $\gamma_{\downarrow\downarrow} \rightarrow 1$ implying that $\gamma_3 = -\gamma_0 \rightarrow 1/2$. Intuitively, one may understand that the Case-II would be significantly different from Case-I both qualitatively and quantitatively. In the Case-II, upon receiving an energy ω ($> 2\Delta$) from an incident photon, one partner of a Cooper-pair moves out of the Fermi sphere, while the other partner remains within the Fermi sphere. Let us consider an elementary process of single photon scattering by a Cooper-pair. Suppose, the Cooper-pair consists of an atom A having spin \downarrow and momentum \mathbf{k} and another atom B with spin \uparrow and momentum $-\mathbf{k}$. When this Cooper-pair is broken due to stimulated scattering of σ_- polarized photon in a situation like Case-II, atom A will move out of the Fermi surface as an excited quasi-particle with momentum $\mathbf{k} + \mathbf{q}$ with certain probability given by BCS correlation and atom B will have certain probability of remaining within the Fermi sphere moving as a quasi-particle with momentum $-\mathbf{k}$. Thus, only one partner of the Cooper-pair will contribute to the intensity of scattered atoms reducing the strength of the density fluctuation spectrum compared to that of Case-I. However, there could be some advantage in detecting the scattered atoms in Case-II by spin-selective time-of-flight measurement technique as we will discuss later in the concluding section.

7.1. Case-I: Leading approximations

In this case, we have $\gamma_0 = 0$. In the limit $\gamma_3 \rightarrow 1$,

$$S_I(\mathbf{q}, \omega) = S_3(\mathbf{q}, \omega) \quad (55)$$

which is given by Eq. (54). For $\beta > 1$, in the leading approximation in terms of β^{-1} , this reduces to the form

$$S_I^{\text{lead}}(\mathbf{q}, \omega) = N(0) \frac{\omega^2}{4\Delta^2} \left\langle \frac{1}{\beta^3 \sqrt{\beta^2 - 1}} \right\rangle, \quad \beta > 1 \quad (56)$$

which is devoid of any vertex correction. The same expression can be derived by taking $\Gamma^{(3)} \rightarrow \gamma_3$, $\Gamma^{(0)} \rightarrow \gamma_0$ and $\Gamma^{(2)} \rightarrow 0$ meaning that we use bare vertex only. This is also obtainable from the static BCS- Bogoliubov mean-field treatment as shown in the appendix. Because of the absence of vertex correction, it violates the Ward identities [48] that guarantee the conservation of total particle number and the obeysance of the continuity equation.

To perform the integration over z in Eq. (56), it is convenient to change the variable into

$$x = \frac{p_q v_k z}{\sqrt{\omega^2 - 4\Delta^2}} \quad (57)$$

The condition $\beta > 1$ implies $x < 1$. Then the Eq. (56) can be expressed as

$$S_I^{\text{lead}}(\mathbf{q}, \omega) = \frac{2N(0)\Delta^2}{\omega p_q v_F} \int_0^{x_0} dx \frac{1}{(1 - jx^2)^{3/2} \sqrt{1 - x^2}} \quad (58)$$

where $j = 1 - 4\Delta^2/\omega^2$ and

$$x_0 = \text{Min} \left[1, \frac{p_q v_F}{\sqrt{\omega^2 - 4\Delta^2}} \right]. \quad (59)$$

For $2\Delta < \omega < \sqrt{(p_q v_F)^2 + 4\Delta^2}$, we have $x_0 = 1$ and the result is

$$S_I^{\text{lead}}(\mathbf{q}, \omega) = \frac{N(0)\omega}{2p_q v_F} E(j), \quad (60)$$

where $E(j)$ is the complete elliptic integral. Note that in the limit $\Delta \rightarrow 0$ $S_I^{\text{lead}}(\mathbf{q}, \omega)$ reduces to the form $N(0)\omega/(2p_q v_F)$ which is same as that of a normal quantum fluid of noninteracting quasi-particles within the energy range $0 < \omega < v_F p_q$ [49]. The dynamic structure factor reaches a maximum at $\omega_0 = \sqrt{(p_q v_F)^2 + 4\Delta^2}$. As ω increases above ω_0 , x_0 decreases below unity and hence the integral in Eq. (58) decreases.

In view of the forgoing analysis, we now verify how far f-sum rule is fulfilled by the dynamic structure factor as given by Eq. (56). To this end, we separate the integral over energy in the sum rule

$$\int \omega S(\mathbf{q}, \omega) d\omega = \int_0^{\omega_0} \dots d\omega + \int_{\omega_0}^{\infty} \dots d\omega. \quad (61)$$

Since Eq. (56) holds good for $\omega > 2\Delta$, the first integral appearing on the right hand side of Eq. (61) results in

$$I_1 = \int_{2\Delta}^{\omega_0} \omega S(\mathbf{q}, \omega) d\omega = \frac{N(0)}{2p_q v_F} \int_{2\Delta}^{\omega_0} \omega^2 E(j) d\omega \quad (62)$$

where we have used the Eq. (60). In the limit $\Delta \rightarrow 0$, $E(j) \rightarrow 1$ and so we obtain

$$I_1 = \frac{N(0)(p_q v_F)^2}{6} = \frac{k_F^3 p_q^2}{3\pi^2 2m} = \frac{N p_q^2}{2m} \quad (63)$$

where we have used $N(0) = (\pi\hbar)^{-2} m k_F$. Here N represents the total number of particle per unit volume. The second integral on the RHS of Eq. (61) is much smaller than

the first one. Thus, we find that in the limit $\Delta \rightarrow 0$, or alternatively, for $p_q v_F \gg 2\Delta$ and $\omega \gg 2\Delta$, that is, for large momentum and energy transfer, the dynamic structure factor as given by Eq. (56) approximately satisfies the f-sumrule. In this context, it may be worthwhile to mention here that for evaluating gap energy from the measurements of the scattering cross section of the light-scattered atoms released from a trap, large momentum transfer is indeed required to distinguish the scattered atoms from the un-scattered ones [42, 50]. For single-particle excitation ($\beta > 1$) with small energy transfer, this leading approximation is not valid and the second term on the RHS of Eq. (54) makes significant contribution resulting from vertex correction. We will show in the appendix that the DSF in leading order approximation is obtainable from BCS-Bogoliubov mean-field treatment that does not take into account final state (quasi-particles) interaction.

7.2. Case-II: Leading approximations

In this case $\gamma_{\uparrow\uparrow} \rightarrow 0$ and $\gamma_{\downarrow\downarrow} \rightarrow 1$ implying $\gamma_0^2 \simeq \gamma_3^2 \neq 0$. Let us use $\gamma_0^2 \simeq \gamma_3^2 \rightarrow 1/4$. Then we have

$$S_{II}(\mathbf{q}, \omega) = \frac{S_0(\mathbf{q}, \omega) + S_3(\mathbf{q}, \omega)}{4}. \quad (64)$$

The angular integration in Eq. (53) can be conveniently performed using the x -variable as already introduced in Eq. (57). Explicitly, this takes the form

$$S_0(\mathbf{q}, \omega) = \frac{2N(0)\Delta^2}{\omega p_q v_F} \int_0^{x_0} dx \frac{jx^2}{(1-jx^2)^{3/2} \sqrt{1-x^2}} \quad (65)$$

where j and x_0 are already defined above. For $2\Delta < \omega < \sqrt{(p_q v_F)^2 + 4\Delta^2}$, $x_0 = 1$ and the result is

$$S_0(\mathbf{q}, \omega) = \frac{2N(0)\Delta^2}{\omega p_q v_F} \frac{\pi j}{4} {}_2F_1(3/2, 3/2; 2, j) \quad (66)$$

${}_2F_1(a, b; c, d)$ is the hypergeometric function. In the limit $\Delta \rightarrow 0$, $\frac{\pi j(1-j)}{4} {}_2F_1 \rightarrow 1$, hence we obtain

$$S_0(\mathbf{q}, \omega) = \frac{N(0)\omega}{2p_q v_F} \quad (67)$$

which again coincides with the form of the DSF of normal fluid within the specified parameter regime.

In passing, we reemphasize that the leading order approximations are valid for $\beta \gg 1$, that is, for large energy transfer. In this limit, $j \rightarrow 1$ and so DSF's in both the cases tend to become equal. All the results followed from leading order approximations can also be obtained with BCS-Bogoliubov mean-field approximation without any vertex correction as illustrated in the appendix.

7.3. Bogoliubov-Anderson mode

Now let us consider the case $0 \leq \beta \ll 1$, that is $\mathbf{v}_k \cdot \mathbf{p}_q \leq \omega \ll 2\Delta$. In this case, the second term in Eq. (44) dominates over all other terms. This term leads to Bogoliubov-Anderson collective phonon mode appearing as a pole in χ . It is evident that the origin of this pole lies in the vertex correction, since this is also the pole of $\Gamma^{(2)}$. The pole is given by

$$\langle [\omega^2 - (\mathbf{v}_F \cdot \mathbf{p}_q)^2] f \rangle = 0. \quad (68)$$

In the limit $q \rightarrow 0$ and $\omega \rightarrow 0$, $f \simeq 1$ and hence the pole is

$$\omega_{BA} = \frac{1}{\sqrt{3}} v_F p_q \quad (69)$$

The BA mode restores the continuous symmetry which is broken by BCS ground state. It is required to fulfill the Ward identities [48]. In the low momentum and low energy limit ($0 \leq \beta \ll 1$) the dynamic structure factor can be obtained by linearizing the denominator of the second term in Eq. (48) around the BA mode. By approximating $f \simeq 1$, we then obtain

$$S(\mathbf{q}, \omega) = N(0) \gamma_3^2 \frac{\omega^2}{2\omega_{BA}} \delta(\omega - \omega_{BA}). \quad (70)$$

With $\gamma_3 \rightarrow 1$, this satisfies the f -sum rule

$$\int_0^\infty \omega S(\omega, \mathbf{q}) d\omega = \frac{Nq^2}{2m} \quad (71)$$

where N is the total number of particles.

To have higher order (in terms of ξq) corrections [51] to the BA mode, we expand the function $f(\beta)$ to the fourth order in β and obtain the result

$$f(\beta) \simeq 1 + \frac{2\beta^2}{3} + \frac{\beta^4}{12} \quad (72)$$

Then the pole is then given by

$$\langle \beta^2 f(\beta) \rangle \simeq \langle \beta^2 + \frac{2\beta^4}{3} \rangle = 0 \quad (73)$$

resulting in

$$\omega_{BA}^2 = \frac{(v_F p_q)^2}{3} \left[1 - \frac{8}{45} \left(\frac{v_F p_q}{2\Delta} \right)^2 \right] \quad (74)$$

BA mode is well defined in the low momentum regime, i.e., for $\xi q = v_F p_q / (2\Delta) \ll 1$. For large momentum, it becomes ill defined due to Landau damping. To get the dynamical correction to BA mode [33, 52], the right hand side of Eq. (74) needs to be multiplied by a factor $[1 - g|a_s|N(0)]$.

Before closing this section, we would like to stress that the polarization-selective small angle stimulated light scattering may be useful in exciting BA mode. Because, unequal momentum and energy transfer can be accomplished by making $\gamma_{\uparrow\uparrow} \neq \gamma_{\downarrow\downarrow}$. This will lead to unequal response of the two spin states. In the small momentum and energy transfer regime, this will result in large wave-length center-of-mass motion of Cooper-pairs and hence superfluid density fluctuation [34]. However, how to detect this BA mode of superfluid trapped atoms is presently unknown.

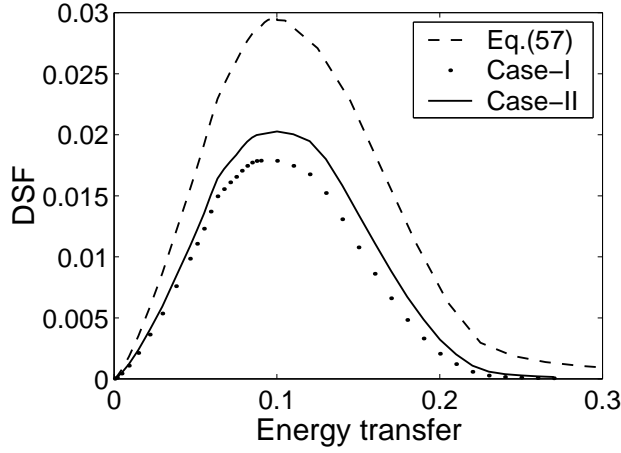


Figure 7. Scaled dimensionless dynamic structure factor (DSF) of superfluid trapped Fermi gas as a function of dimensionless energy transfer (ω/ϵ_F) for different cases (see the text). For the sake of comparison, DSF for the two cases are scaled differently: $S_I(\omega, \mathbf{q})$ and $S_{II}(\omega, \mathbf{q})$ are scaled by the factors $1/[2N(0)]$ and $1/N(0)$, respectively. The momentum transfer is kept fixed at $q/k_F = 0.2$. The scattering length is $a_s = 0.51k_F^{-1}$ for which the BCS gap Eq. (76) yields the value of the gap at the trap center as $\Delta_0 = 0.05\epsilon_F$. Case-I (dotted) refers to the unpolarized light in the absence of magnetic field, case-II refers to the circularly polarized light in the presence of magnetic field. Dashed curve (Eq. (57)) is for unpolarized light without vertex correction when only BCS-type mean-field is used.

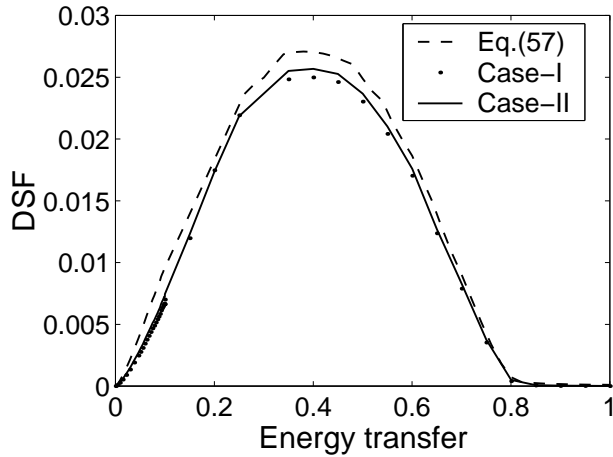


Figure 8. Same as in Fig. 1 but for $q = 0.8k_F$

8. Numerical results and discussion

We now apply the formalism discussed above to harmonically trapped superfluid Fermi atoms. For simplicity, we consider an isotropic optical trap characterized by the length scale $a_{ho} = \sqrt{\hbar/(m\omega_{ho})}$, where ω_{ho} is the trapping frequency. In Thomas-Fermi local density approximation (LDA) [53], the state of the system is governed by

$$\epsilon_F(\mathbf{r}) + V_{ho}(\mathbf{r}) + U(\mathbf{r}) = \mu, \quad (75)$$

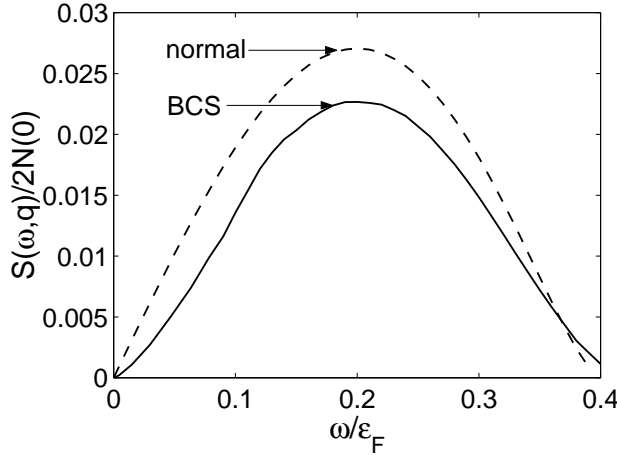


Figure 9. DSF of BCS superfluid (solid) and normal fluid (dashed) are plotted as a function of energy transfer for $q = 0.4k_F$ and $\Delta_0 = 0.05$ for the case-I.

where $\epsilon_F(\mathbf{r}) = \hbar^2 k_F(\mathbf{r})^2 / (2m)$ is the local Fermi energy, $k_F(\mathbf{r})$ denotes the local Fermi momentum which is related to the single-spin local number density by $n(\mathbf{r}) = k_F(\mathbf{r})^3 / (6\pi^2)$. Here U represents the mean-field interaction energy and μ is the chemical potential. At low energy, the mean-field interaction energy depends on the two-body s-wave scattering amplitude $f_0(k) = -a_s / (1 + ia_s k)$, where a_s represents s-wave scattering length and k denotes the relative wave number of two colliding particles. In the dilute gas limit ($|a_s|k \ll 1$), U becomes proportional to a_s in the form $U(\mathbf{r}) = \frac{4\pi\hbar^2 a_s}{2m} n(\mathbf{r})$. In the unitarity limit $|a_s|k \rightarrow \infty$, the scattering amplitude $f_0 \sim i/k$ and hence U becomes independent of a_s . It then follows from a simple dimensional analysis that in this limit, U should be proportional to the Fermi energy: $U(\mathbf{r}) = \beta_u \epsilon_F(\mathbf{r})$ where β_u is the constant. In this limit, the pairing gap also becomes proportional to the Fermi energy. Based on the regularized mean-field approach discussed earlier and LDA, the zero-temperature density profiles [54], momentum distribution [55] and the finite temperature effects [56] of superfluid trapped Fermi atoms have been recently studied. For dilute gas limit, the local density distribution of trapped gas may be approximated by neglecting the interaction term U in Eq. (75). In the BCS limit ($k_F a_s \rightarrow 0^-$), the gap is exponentially small and can be expressed by the well known formula

$$\Delta_{\text{BCS}} \simeq \frac{8\epsilon_F}{e^2} \exp\left[-\frac{\pi}{2k_F |a_s|}\right], \quad (76)$$

where ϵ_F is the Fermi energy.

Under LDA, the density profile of a trapped Fermi gas is given by

$$n(\mathbf{r}) = n(\mathbf{0})(1 - r^2/R_{TF}^2)^{3/2}, \quad (77)$$

where $n(\mathbf{0}) = 1/(6\pi^2\hbar^3)[2m\mu/(1 + \beta_u)]^{3/2}$ is the density of the atoms at the trap center. Here $R_{TF}^2 = 2\mu/(m\omega_{ho}^2)$ is the Thomas-Fermi radius of the trapped atomic gas. The normalization condition on Eq. (77) gives an expression for $\mu = (1 + \beta_u)^{1/2}(6N_\sigma)^{1/3}\hbar\omega_{ho}$ where N_σ is the total number of atoms in the hyperfine spin σ . The Fermi momentum

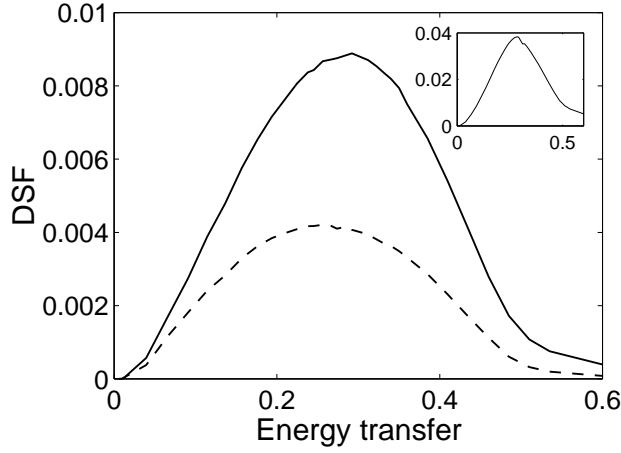


Figure 10. Dimensionless scaled DSF $S_I(\omega, \mathbf{q})/(2N(0))$ (dashed) and $S_{II}(\omega, \mathbf{q})/N(0)$ Vs. dimensionless energy transfer ω/ϵ_F for $q = 0.4k_F$ and $a_s = 3.21k_F^{-1}$. For this larger scattering length, using the regularized gap Eq. (36), the gap is calculated to be $\Delta_0 = 0.15\epsilon_F$. The inset shows the corresponding plot in Case-I for leading order approximation as given Eq. (57).

at the trap center $k_F^0 = [3\pi^2 n(\mathbf{0})]^{1/3} = (1 + \beta_u)^{-1/4} k_F$ where $k_F = (48N_\sigma)^{1/6}/a_{ho}$ is the Fermi momentum of the noninteracting trapped gas. Under LDA, the dynamic structure factor is given by

$$S(\mathbf{q}, \omega) = \frac{1}{V_{TF}} \int d^3\mathbf{r} S_r(\mathbf{q}, \omega) \quad (78)$$

where $S_r(\mathbf{q}, \omega)$ is the DSF for Fermi momentum $k_F(\mathbf{r})$ evaluated at a position \mathbf{r} assuming the system is locally uniform. Here $V_{TF} = (4/3)\pi R_{TF}^3$ is the Thomas-Fermi volume.

In Figs. 7-10, we show DSF (calculated using LDA) of superfluid trapped Fermi gas due to single-particle excitations only as a function of energy transfer under different physical conditions. Figs. 7-9 are plotted for $a_s k_F < 1$ with gap given by BCS gap Eq. (76) while Fig. 10 is for $a_s k_F > 1$ with gap determined by the regularized gap Eq. (36) coupled with the superfluid number Eq. (37). For the sake of better comparison, we have scaled the DSF in Case-II (denoted by S_{II} hereafter) by a factor $[N(0)]^{-1}$ while DSF in Case-I (denoted by S_I hereafter) is scaled by half of this factor, that is, by $[2N(0)]^{-1}$. Here $N(0)$ refers to the density of states at the trap center. By comparing Fig. 7 and Fig. 8 which are plotted for lower and higher momentum transfer, respectively, we infer that the vertex correction is most significant in low momentum and energy transfer regime. At high momentum and energy transfer regime, mean-field approximation seems to be reasonably good. Furthermore, at lower momentum transfer, S_{II} shows larger deviation from $S_I/2$ with both tending to equalize at higher energy transfer.

In Fig. 9, we compare DSF of superfluid gas with corresponding DSF for normal fluid. The two curves do not show any discernible shift of their peak values apparently due to exponentially small gap. However, as ω decreases below the value at which the maxima occurs, DSF in superfluid case exhibits reducing gradient in contrast to that of normal case of almost steady gradient. This feature may constitute an indication

of the occurrence of BCS-type superfluidity in trapped Fermi gas. This feature can be explained on the basis of inhomogeneous density distribution of trapped gas. For a uniform Fermi superfluid, in the single-particle excitation regime, DSF remains zero until energy transfer exceeds 2Δ at which it rises sharply with the increasing energy transfer. For a superfluid trapped Fermi gas, owing to the spatial distribution of the gap, DSF has a structure below $2\Delta_0$, where Δ_0 represents the gap at the trap center. As ω goes to zero, the gradient of $S(\delta, \mathbf{q})$ vanishes. In the low energy regime ($\omega < 2\Delta_0$), $S(\omega, \mathbf{q})$ varies with ω nonlinearly. When ω approaches $2\Delta_0$, the gradient changes abruptly implying a discontinuity (which may be indiscernible experimentally on practical grounds). This behavior can also be explained by considering the boundary condition $2\Delta(\mathbf{x}) < \omega$. This spatially dependent lower bound on ω implies that, when ω is less than $2\Delta_0$, the atoms at the central region of the trap can not respond to the light fields via single-particle excitations, only those atoms in the peripheral region can do so.

Fig. 10 displays DSF for both the Case-I and Case-II for larger scattering length $a_s = 3.21k_F^{-1}$ for which the gap is $\Delta_0 = 0.15\epsilon_F$. For both the Figs. 9 and 10, q is fixed at $0.4k_F$. In comparison to the Fig. 9, we notice that the peak of DSF in Fig. 10 exhibits a shift apparently due to the occurrence of relatively larger gap. We further notice that the width has been broader with peak value reduced by roughly one order of magnitude. This may be attributed to the relatively larger interaction and hence larger vertex correction.

9. conclusion

In conclusion we have presented a detailed theoretical analysis of the response of Cooper-paired Fermi atoms due to off-resonant light scattering at zero temperature. We have studied vertex correction which is quite significant at low momentum. By making use of the Zeeman shifts between two ground hyperfine spin states and also between the excited state hyperfine spin manifolds, we have shown that it is possible to transfer different amount of momentum and energy to the two partner atoms of a Cooper pair. Light polarization plays an important role in selective single-particle excitations in superfluid Fermi atoms. Using circularly polarized light in the presence of a magnetic field, quasi-particle excitation can be obtained in one spin component only. We have analyzed the dynamic structure factor (DSF) due to single-particle excitations under different physical conditions. DSF shows a shift for large gap. In contrast to trapped normal Fermi atoms, the gap inhomogeneity of trapped Cooper-paired Fermi atoms leads to relatively reduced gradient of DSF below $2\Delta_0$, where Δ_0 is the gap at the trap center. This reducing gradient may constitute a signature of superfluid state.

Although the focal theme of this paper has been the theoretical analysis of stimulated scattering of polarized light by superfluid Fermi atoms under different physical conditions, there is some relevance of it in experiments with Fermi atoms. The question arises how to detect experimentally spectrum of density fluctuation (or DSF) of superfluid two-component Fermi atoms such as ${}^6\text{Li}$. Towards this end, we wish

to present some speculative and suggestive discussions. We recall that the DSF of BEC has been experimentally detected [35, 58] using stimulated light scattering (or Bragg spectroscopy) and the well-established method of time-of-flight measurements. One of the major difficulties in evaluating DSF of two-component Fermi atoms from time-of-flight measurements might stem from the fact that the initial information about the momentum distribution of the atoms may be washed away during expansion due to relatively large s-wave collisions of the two hyperfine spin components. This difficulty can be circumvented by the method of rapidly reducing the magnetic field (that induces Feshbach resonance) just before switching off the trap as done in numerous recent experiments [9, 14, 24]. In light scattering experiment, polarization-selective light scattering may be useful in suppressing the collisions among the scattered atoms during their expansion on being released from the trap. Since the scattered atoms will be in a single spin state, there will be diminished probability of collision among those atoms (the leading order p-wave collision at low temperature is vanishingly small). This may lead to better precision in time-of-flight spin-selective measurements [23, 57] of scattered atoms. Order of magnitude analysis of Ref. [42] suggests that, with large momentum transfer, it may be possible to distinguish the scattered atoms in time of flight images. To reveal the information about the momentum and density distribution of scattered atoms, the time-of-flight images with and without Bragg pulses should be compared. Furthermore, Bragg spectroscopy allows one to choose different directions for scattered atoms, since the scattering is of predominantly stimulated type. It may be possible to scatter atoms in two opposite directions by using three or four beam stimulated light scattering configuration as discussed in [42]. One can then explore the possibility of measuring the correlation of two scattered atoms with opposite momentum by similar technique as applied in recent theoretical [59] and experimental [60] studies. Finally, polarization-selective light scattering may be useful in exciting BA mode the detection of which poses a challenging experimental problem.

Appendix

We here present an alternative derivation of DSF without vertex correction using BCS-Bogoliubov mean-field treatment. This DSF coincides with that obtained using leading approximation as described in the text. It can be defined by $S(\mathbf{q}, \omega) = \sum_f |\langle f | \sum_{\sigma=\uparrow, \downarrow} \gamma_{\sigma\sigma} \rho_{\sigma}^{\dagger}(\mathbf{q}) | 0 \rangle|^2 \delta(\omega - \epsilon_f + \epsilon_0)$ where $|0\rangle$ represents the many-body ground state with energy ϵ_0 and the sum runs over all the final states $|f\rangle$ which can be coupled to the ground state by the density operator $\rho_{\sigma}(\mathbf{q}) = \sum_{\mathbf{k}} a_{\sigma, \mathbf{k}+\mathbf{q}}^{\dagger} a_{\sigma, \mathbf{k}}$. The DSF for the Case-I, that is, for the condition $\gamma_{\uparrow\uparrow} = \gamma_{\downarrow\downarrow}$ has been explicitly calculated in Ref. [37]. We here assume $\gamma_{\uparrow\uparrow} \neq \gamma_{\downarrow\downarrow}$, and as an extreme case we consider the case-II: $\gamma_{\uparrow\uparrow} \simeq 0$ and $\gamma_{\downarrow\downarrow} \rightarrow 1$. Setting $\epsilon_0 = 0$, we can write

$$S(\mathbf{q}, \omega) = \frac{V}{(2\pi)^3} \int d^3k n_k (1 - n_{k'}) \delta(\omega - E_{k'} - E_k) \quad (\text{A.1})$$

where $k' = |\mathbf{k} + \mathbf{q}|$ is the wave number of a scattered atom, V is the volume of the system and $n_k = v_k^2 = (1 - \xi_k/E_k)/2$ is the momentum distribution function. Here $E_k = \sqrt{\xi_k^2 + \Delta_k^2}$ is the energy of an elementary excitation (Bogoliubov's quasiparticle), Δ_k represents the pairing gap and $\xi_k = \hbar^2 k^2/(2m) - \mu$. Note that the usual BCS coherence factor [37, 44] $m(\mathbf{k}, \mathbf{k}') = u_{k'}v_k + u_kv_{k'}$ where $u_k^2 = 1 - v_k^2$, has changed. This is due to the fact that the momentum and energy transfer occurs in either partner of a Cooper pair because of polarization-selective light scattering.

We here give an outline of the method of calculation of the integral in Eq. (A.1). For notational simplicity, we denote $\xi = \xi_k$ and $\xi' = \xi_{k'} \simeq \xi + \mathbf{v}_k \cdot \mathbf{p}_q$; and similarly we replace E_k and $E_{k'}$ by E and E' , respectively. The integration may be restricted near $\xi = \epsilon_k - \mu \simeq 0$, since the dominant contribution to the integration comes from k -values near $\epsilon_k \simeq \mu$. For convenience, we change the variable of integration into E by using the relation $d\xi = EdE/(E^2 - \Delta^2)^{1/2}$. Using the identity

$$\delta(\omega - E - E') = \frac{\delta(E - E_0)}{|(1 + dE'/dE)|_{E=E_0}} \quad (\text{A.2})$$

where E_0 is the solution of the equation $E + E' = \omega$, we have

$$S(\mathbf{q}, \omega) = \frac{V}{(2\pi)^3} \int d^3\mathbf{k} \delta(\xi_k) \left[\frac{(E - \xi)(E' + \xi')}{4 |1 + dE'/dE| \xi E'} \right]_{E=E_0}. \quad (\text{A.3})$$

After a lengthy algebra as in Ref. [37], we then obtain

$$S(\mathbf{q}, \omega) = \frac{V}{(2\pi)^3} \int d^3\mathbf{k} \delta(\xi_k) \frac{(\omega + \mathbf{p}_q \cdot \mathbf{v}_k)^2}{16\Delta^2 \beta^3 \sqrt{\beta^2 - 1}}, \quad (\text{A.4})$$

where β is defined in Eq. (28). Let $z = \cos \theta$, where θ is the angle between \mathbf{k} and \mathbf{q} . Changing the variable of angular integration into $x = v_k p_q z / \sqrt{\omega^2 - 4\Delta^2}$, one obtains

$$S(\mathbf{q}, \delta) = \frac{N(0)\Delta^2}{2p_q v_F \omega} \int_0^{x_0} dx \frac{(1 + jx^2)}{(1 - jx^2)^{3/2} \sqrt{1 - x^2}}, \quad (\text{A.5})$$

where $j = 1 - 4\Delta^2/\omega^2$ and $x_0 = \text{Min} \left[1, \frac{p_q v_F}{(\omega^2 - 4\Delta^2)^{1/2}} \right]$. In writing the above equation, we have considered the weak-coupling case and hence replaced the chemical potential μ by the Fermi energy ϵ_F . If $2\Delta < \omega < (p_q v_F)^2 + 4\Delta^2)^{1/2}$, then $x_0 = 1$ and the result is

$$S(\mathbf{q}, \delta) = \frac{N(0)\omega}{8p_q v_F} [E(j) + M {}_2F_1(3/2, 3/2; 2, j)] \quad (\text{A.6})$$

where $M = \pi j(1 - j)/4$. Here $E(j)$ represents the complete elliptic integral and ${}_2F_1(a, b; c, d)$ is the hypergeometric function. In the limit $\Delta \rightarrow 0$, $E(j) \rightarrow 1$ and $M {}_2F_1 \rightarrow 1$ leading to the result $S(\delta, \mathbf{q}) = \nu_F \delta / (4p_q v_F)$ which is half the dynamic structure factor of normal fluid [49] consisting of noninteracting quasi-particles within the specified energy range. The factor half arises due to our initial assumption $\gamma_{\uparrow\uparrow} \simeq 0$ and $\gamma_{\downarrow\downarrow} \rightarrow 1$ which implies that only spin \downarrow are scattered and since the number of atoms in the two spin components are assumed to be equal, only half of the total number of atoms contribute to the scattered flux of atoms.

References

- [1] Cohen-Tannoudji C. 1998 *Rev. Mod. Phys.* **70** 707; Chu S. 1998 *ibid* **70** 685 ; Philips W. D. 1998 *ibid* **70** 721
- [2] Anderson M., Ensher J. R., Matthews M. R., Wieman C. E., and Cornell E. A. 1995 *Science* **269** 198; Bradley C. C., Sackett C. A., Tollett J. J. , and Hulet R. G. 1995 *Phys. Rev. Lett.* **75** 1687 ; Davis K. B. , Mewes M. O., Andrews M. R., van Druten N. J., Durfee D. S., Kurn D. M. , and Ketterle W. 1995 *Phys. Rev. Lett.* **75** 3969
- [3] Einstein A. 1924 *Sitzber. Kgl. Preuss. Akad. Wiss.* 261 1925 *ibid* 3
- [4] Bose S. N. 1924 *Z. Phys.* **26** 178.
- [5] Stoof H. T. C., Houbiers M., Sackett C. A., and Hulet R. G. 1996 *Phys. Rev. Lett.* **76** 10; M. Houbiers *et al.* 1997 *Phys. Rev. A* **56** 4864 ; DeMarco B. and Jin D. S. 1998 *Phys. Rev. A* **58** 4267
- [6] Heiselberg H. 2001 *Phys. Rev. A* **63**, 043606 ; H. Heiselberg, C. J. Pethik, H. Smith, and Viverit L. 2000 *Phys. Rev. Lett.* **85** 2418; Bruun G. M. and Heiselberg H. 2003 *Phys. Rev A* **65** 053407
- [7] B. DeMacro and D. S. Jin 1999 *Science* **285** 1703
- [8] A. G. Truscott, K. E. Strecker, W. I. McAlexander, G.B. Patridge, and R. G. Hulet 2001 *Science* **291** 2570
- [9] F. Schreck *et al.* 2001 *Phys. Rev. Lett.* **87** 080403; T. Bourdel *et al.* 2003 *ibid.* **91** 020402
- [10] S. R. Granade, M. E. Gehm, K. M. O'Hara, and J. E. Thomas 2002 *Phys. Rev. Lett.* **88**, 120405; O'Hara *et al.* 2002 *Science* **298** 2179
- [11] Z. Hadzibabic *et al.*, *Phys. Rev. Lett.* **88**, 160401 (2002).
- [12] G. Roati, F. Riboli, G. Modugno, and M. Inguscio, *Phys. Rev. Lett.* **89**, 150403 (2002).
- [13] Jochim S. *et al.* 2003 *Science* **302** 2101
- [14] Zwierlein M. W., Abo-Shaer J. R., Schirotzek A., Schunck C. H., Ketterle W. 2005 *Nature* **435** 1047
- [15] Cin C. *et al.* 2004 *Science* **305** 1128
- [16] Greiner M., Regal C. A., and Jin D. S. 2005 *Phys. Rev. Lett.* **94** 070403
- [17] Kinast, J. *et al.* 2004 *Phys. Rev. Lett.* **92** 150402
- [18] Bartenstein M. *et al.* 2004 *Phys. Rev. Lett.* **92** 203201
- [19] Stringari S. 2004 *Europhys. Lett.* **65** 749
- [20] Nozières P. and Schmitt-Rink S. 1985 *J. Low. Temp. Phys.* **59** 195
- [21] Sa de Melo C.A.R., Randeria M. and Engelbrecht J.R. 1993 *Phys. Rev. Lett.* **71** 3202; Engelbrecht J.R., Randeria M. and Sa de Melo C.A.R. 1997 *Phys. Rev. B* **55** 15153
- [22] Holland M., Kokkelmans S. J. J. M. F., Chiofalo M. L. and Wasler R. 2001 *Phys. Rev. Lett.* **87** 120406; Timmermans E. *et al.* 2001 *Phys. Lett A* **285** 228; Ohashi Y. and Griffin A. 2002 *Phys. Rev. Lett.* **89** 130402; Hofstetter W. *et al.* 2002 *Phys. Rev. Lett.* **89** 220407
- [23] Greiner M., Regal C. A. and Jin D. S. 2003 *Nature* **426** 537; Jochim S. *et al.* 2003 *Science* **302** 2101; Zwierlein M. W. *et al.* 2003 *Phys. Rev. Lett.* **91** 250401
- [24] Modugno G. *et al.* 2002 *Science* **297** 2240; Strecker K. E. *et al.* 2003 *Phys. Rev. Lett.* **91** 080406; Cubizolles J. *et al.* 2003 *Phys. Rev. Lett.* **91** 240401
- [25] Falco G. M. and Stoof H. T. C. 2004 *Phys. Rev. Lett.* **92** 130401; Carr L. D., Shlyapnikov G. V. and Castin Y. 2004 *Phys. Rev. Lett.* **92** 150404; Heiselberg H. 2003 *Phys. Rev. A* **68** 053616, Perali A., Pieri P. and Strinati G. C. 2003 *Phys. Rev. A*, **68** 031601; Perali A., Pieri P., Pisani L. and Strinati G. C. *lanl e-print cond-mat/0311309*.
- [26] Törmä P. and Zoller P. 2000 *Phys. Rev. Lett.* **85** 487; Bruun G. M. *et al.* 2001 *Phys. Rev. A* **64** 033609; Kinnunen J., Rodriguez M., and Törmä P 2004 *Phys. Rev. Lett.* **92** 230403; Bruun G. M. and Baym G. 2004 *Phys. Rev. Lett.* **93** 150403; Büchler H. P., Zoller P., Zwerger W. 2004 *Phys. Rev. Lett.*, **93** 080401
- [27] Kinnunen J., Rodriguez M., and Törmä P 2004 *Science* **305** 1131
- [28] Zhang W., Sackett C. A. and Hulet R. G. 1999 *Phys. Rev. A* **60** 504; Ruostekoski J. 1999 *Phys.*

- Rev. A* **60** 1775; Rodriguez M. and Törmä P. 2002 *Phys. Rev. A* **66** 033601.
- [29] Bruun G. M. and Mottelson B. R. 2001 *Phys. Rev. Lett.* **87** 270403
- [30] Ohashi Y. and Griffin A. 2003 *Phys. Rev. A* **67** 063612; Ohashi Y. and Griffin A. *lanl archive cond-mat/0503641*
- [31] Minguzzi A., Ferrari G. and Castin Y. 2001 *Eur. Phys. J. D.* **17** 49
- [32] Bogoliubov N. N. 1958 *Nuovo Cimento* **7** 6; Bogoliubov N. N., Tolmachev V. V., and Shirkov D. V. 1959 *A New Method in the Theory of Superconductivity* (Consultants Bureau, NY).
- [33] Anderson P. W. 1958 *Phys. Rev.* **112** 1900
- [34] Martin P. C., in 1969 *Superconductivity*, Vol.1, edited by Parks R. D. (Dekker, NY).
- [35] Stenger J. *et al.* 1999 *Phys. Rev. Lett.* **82** 4569; Ketterle W. and Inouye S., *lanl e-print cond-mat/0101424*.
- [36] Abrikosov A. A. and Fal'kovskii L. A. 1961 *Soviet Physics JETP* **13** 179
- [37] Klein M. V. and Dierker S. B. 1984 *Phys. Rev. B* **29** 4976
- [38] Nambu Y. 1960 *Phys. Rev.* **117** 648
- [39] Abrikosov A. A., Gorkov L. P., and Dzyaloshinski 1963 *Methods of Quantum Field Theory in Statistical Physics* (Dover, NY).
- [40] Sakurai J. J. 1967 *Advanced Quantum Mechanics* (Pearson Education, Inc.)
- [41] W. V. Liu and F. Wilczek 2003 *Phys.Rev.Lett.* **90** 047002
- [42] Deb B., Mishra A., Mishra H. and Panigrahi P. K. 2004 *Phys. Rev. A* **70** 011604
- [43] Gupta S. *et al.* 2003 *Science* **300** 1723
- [44] Schrieffer J. R. 1964 *Theory of Superconductivity* (W. A. Benjamin)
- [45] Feynman R. P. 1951 *Phys. Rev.* **84** 108
- [46] Vaks V. G., Galitskii, and Larkin A. I. 1962 *Soviet Physics JETP* **14** 1177
- [47] Marini M., Pistolesi F. and Strinati G. C. 1998 *Eur. Phys. J. B* **1** 151
- [48] Ward J. C., 1950 *Phys. Rev.* **78** 182
- [49] Pines D. and Nozières P. 1989 *The Theory of Quantum Fluids*, Vol.I (Addison-Wesley)
- [50] Deb B. *LANL e-print archive cond-mat/0505692*
- [51] Angelis G. F. D. and Mancini F. 1974 *Nuovo Cimento* **10** 654
- [52] Amvbeaokar V. and Kadanoff L. P. 1961 *Nuovo Cimento* **22** 914
- [53] Houbiers M. *et al.* 1997 *Phys. Rev. A* **56** 4864; Vichi L. and Stringari S. 1999 *Phys. Rev. A* **60** 4734
- [54] Perali A. Pieri P. and Strinati G. C. 2003 *Phys. Rev. A* **68** 031601
- [55] Viverti L., Giorgini S., Pitaevskii L. P. and Stringari S. 2004 *Phys. Rev. A* **69** 013607
- [56] Perali A. Pieri P., Pisani L. and Strinati G. C. 2004 *Phys. Rev. Lett* **92** 110401
- [57] Regal C. A., Greiner M. and Jin D. S. 2004 *Phys. Rev. Lett.* **92** 040403; Zwierlein M. W., Stan C. A., Schunck C. H., Raupack S. M. F., Kerman A. J. and Ketterle W. 2004 *Phys. Rev. Lett.* **92** 120403
- [58] Stamper-Kurn D. M. *et al.* 1999 *Phys. Rev. Lett.* **83** 2876; Vogels J. M. *et al.* 2002 *Phys. Rev. Lett.* **88** 060402
- [59] Altman E. Demler E., Lukin M. D. 2004 *Phys. Rev. A* **70** (2004) 013603
- [60] Greiner M., Regal C. A., Stewart J. T. and Jin D. S. 2005 *Phys. Rev. Lett.* **94** 110401